

Hot Photoluminescence in γ -In₂Se₃ Nanorods

M. D. Yang · C. H. Hu · J. L. Shen ·
S. M. Lan · P. J. Huang · G. C. Chi ·
K. H. Chen · L. C. Chen · T. Y. Lin

Received: 10 July 2008 / Accepted: 11 September 2008 / Published online: 30 September 2008
© to the authors 2008

Abstract The energy relaxation of electrons in γ -In₂Se₃ nanorods was investigated by the excitation-dependent photoluminescence (PL). From the high-energy tail of PL, we determine the electron temperature (T_e) of the hot electrons. The T_e variation can be explained by a model in which the longitudinal optical (LO)-phonon emission is the dominant energy relaxation process. The high-quality γ -In₂Se₃ nanorods may be a promising material for the photovoltaic devices.

Keywords InSe nanorods · Hot photoluminescence · Energy relaxation

Introduction

The III–VI semiconductors have been the subject of many investigations due to their peculiar electrical and optical properties, and their potential applications in electronic and optoelectronic devices [1–4]. Among these semiconductors, γ -In₂Se₃ has attracted attention because it is suitable for use in photovoltaic applications [5]. In the recent years, many researchers have been interested in the synthesis of the nanoscale materials due to their unique properties and novel applications in optoelectronic and electronic devices [6–8]. Although some progress has been achieved regarding the growth and characterization of γ -In₂Se₃ epilayers, the γ -In₂Se₃ nanostructures have not been grown and investigated yet. The γ -In₂Se₃ nanostructures may show potential applications in optoelectronic device such as lasers, light emitting diodes (LEDs), and solar cells, due to their high surface-to-volume ratio.

When excess energy is supplied to a carrier by optical excitation or an applied electric field, the energetic carrier becomes hot. The hot carriers then relax toward less energetic state by two competing processes, namely scatterings with other carriers and emission of phonons [9]. The understanding of this energy relaxation process constitutes a direct probe of a very fundamental interaction in condensed matter physics, namely, the electron–phonon and electron–electron interactions. Also, the subject is of obvious technological significance since many devices work mostly in high-field conditions. High electric fields may lead to carrier heating and, consequently, transport effects related to the hot carrier distribution function. A knowledge of hot carrier relaxation mechanisms is thus essential not only for understanding the fundamental process in semiconductor materials but also for evaluating optical device performance.

M. D. Yang · C. H. Hu · J. L. Shen (✉)
Department of Physics, Chung Yuan Christian University,
Chung-Li, Taiwan
e-mail: jlshen@cycu.edu.tw

S. M. Lan
Institute of Nuclear Energy Research, Longtan, Taoyuan 32546,
Taiwan

P. J. Huang · G. C. Chi
Department of Physics, National Central University,
Chung-Li 320, Taiwan

K. H. Chen
Institute of Atomic and Molecular Sciences Academia Sinica,
Taipei, Taiwan

L. C. Chen
Center of Condensed Matter Science, National Taiwan
University, Taipei, Taiwan

T. Y. Lin
Institute of Optoelectronic Sciences, National Taiwan Ocean
University, Keelung, Taiwan

In this study, the single phase γ - In_2Se_3 nanorods on silicon (111) substrates were grown by metal-organic chemical vapor deposition (MOCVD). The excitation power dependence of photoluminescence (PL) in γ - In_2Se_3 nanorods was studied. The high-energy tails of the low-temperature PL were characterized by effective electron temperatures which increase with increasing excitation intensity. It is found the main path of energy relaxation of the hot electrons in the γ - In_2Se_3 nanorods is the LO-phonon emission.

Experiment

The γ - In_2Se_3 nanorods were grown on Si (111) substrates by using an MOCVD system at atmospheric pressure with a vertical reactor. The liquid MO, a TMI compound, and gaseous H_2Se were employed as the reactant source materials for In and Se, respectively. The gaseous N_2 was used as the carrier gas in the process. The substrates used in this experiment were cut from a 6-inch *p*-type vicinal (111)-oriented Si wafer. Before the growth, Si substrates were baked at 1100 °C for 10 min in gaseous HCl and H_2 to remove the native oxide. After the thermal etching process, the reactor was cooled down to 425 °C and the γ - In_2Se_3 started to grow. The gaseous flow rate of TMI was kept at 3 $\mu\text{mol}/\text{min}$ and that of H_2Se was controlled at 40 $\mu\text{mol}/\text{min}$. The gaseous H_2Se was mixed with 85% hydrogen and 15% H_2Se . The γ - In_2Se_3 nanorods were grown at 425 °C during a total growth time of 50 min. The structure of the γ - In_2Se_3 nanorods was examined by the X-ray diffraction (XRD) in a θ - 2θ geometry. The XRD measurements were performed by using the $\text{CuK}\alpha$ -radiation ($\lambda = 1.541 \text{ \AA}$) to test the phases of samples. PL was made using the Ar-ion laser operating at a wavelength of 514.5 nm. The room-temperature PL measurements were performed using a confocal microscopy. The collected luminescence was dispersed by a 0.75 m spectrometer and detected with a photo-multiplier tube (PMT).

Results and Discussion

The morphology of the grown γ - In_2Se_3 nanorods was investigated by the scanning electron microscopy (SEM). The cross-sectional image of SEM for the γ - In_2Se_3 nanorods is shown in Fig. 1, indicating a high density and narrow size distribution. The crystallographic face of each nanorod is shown in the inset of Fig. 1, revealing the hexagonal top end of the γ - In_2Se_3 nanorods. The inset of Fig. 2 shows the XRD pattern of γ - In_2Se_3 nanorods. A high intensity of the XRD pattern from the Si (111) plane was clearly observed at $2\theta = 28.44^\circ$. Furthermore, the XRD

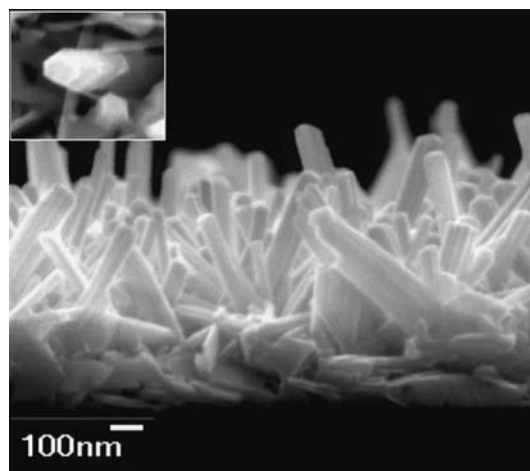


Fig. 1 The γ - In_2Se_3 nanorods morphology obtained by the cross-section SEM image. The inset shows the top-view SEM image

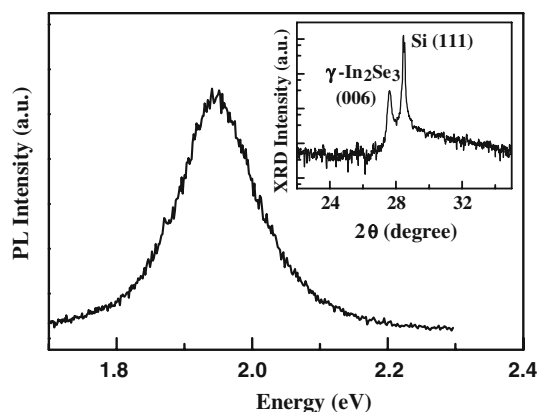


Fig. 2 Room-temperature PL of the γ - In_2Se_3 nanorods. The inset shows the XRD pattern of the γ - In_2Se_3 nanorods

reflection from the plane of γ - In_2Se_3 was also observed at $2\theta = 27.59^\circ$, confirming the hexagonal single phase for the γ - In_2Se_3 nanorods [10]. The 300-K PL spectrum of the γ - In_2Se_3 nanorods is shown in Fig. 2. A clear PL peak was observed with the peak position of 1.95 eV, corresponding to the near band gap edge emission [11]. Observation of the room-temperature luminescence of the γ - In_2Se_3 nanorods indicates the good quality of our sample.

In the process of the hot PL, the photoexcitation creates energetic electrons in the conduction band, which relax toward less energetic state by transferring energy to the lattice (via the electron–phonon scattering) and other electrons (via the electron–electron scattering). If the electron–electron collision rate is larger than the phonon emission rate, then the non-equilibrium electron population in the electron gas relaxes toward a Maxwell distribution and can be characterized by an T_e (T_e) which is higher than the lattice temperature (T_l) [12]. Figure 3(a–d) shows the high-energy tail of the 15-K PL in γ - In_2Se_3 nanorods with

different excitation power densities. The spectra show that the high-energy tail of each PL decreases exponentially with photon energy, revealing that the PL is related to the hot carrier recombination. The high-energy tail of each PL in Fig. 3 can be analyzed by the function [6]:

$$I(\hbar\omega) \sim \exp(-\hbar\omega/E_0), \tag{1}$$

where E_0 is the specific energy. With low excitation power, E_0 reflects the sample quality at low temperatures [6]. Under higher photoexcitation, E_0 can reflect the kinetic energy of the thermalized electrons and a well-defined T_e can be extracted. We have fitted the high-energy tail of PL using Eq. 1, as shown by the solid lines in Fig. 3.

The inverse T_e versus the excitation power is plotted as the open squares in Fig. 4. The slope of the inverse T_e , displayed as the solid line, corresponds to a value of 19 meV. To find out whether this energy is related to the phonon energy in γ -In₂Se₃ nanorods, we performed the Raman scattering measurements. Figure 4 is the Raman spectrum of γ -In₂Se₃ nanorods, displaying a clear peak located at 152 cm⁻¹, whose energy corresponds to ~ 19 meV. Thus, the energy extracted from the slope of the inverse T_e is in good agreement with the phonon energy measured from the Raman scattering. This indicates the phonon scattering is very efficient in transferring energy from electrons to the lattice. In other words, the phonon emission is the dominant energy loss mechanism in the energy relaxation processes of hot electrons in γ -In₂Se₃ nanorods.

To obtain the energy loss rate per electron from experiments, the power balance equations were used. As the steady-state electron population increases by increasing the excitation density, enhanced electron–electron scattering results in a larger fraction of the available energy being shared with the electron gas. Thus, the T_e is determined by balancing the rate of generation for the energetic electrons with the rate of energy loss from the electrons to the lattice. For the photoexcitation, the pump power per electron P_e given to the electron is [12]

$$P_e = \frac{I W 1}{d \hbar\nu_0 n}, \tag{2}$$

where I is the laser power absorbed per unit area, d is the absorption length at laser energy, n is the carrier concentration, and W is the part of the photon excess energy obtained by electron. The carrier concentration n was obtained from the room-temperature Hall-effect measurements. The open square in Fig. 5 displays the T_e as a function of the power input per electron (P_e). If we assume the dominant process for this relaxation is through LO-phonon emission and T_e is much larger than T_l , then the energy loss rate per electron due to the LO-phonon scattering can be given by [13].

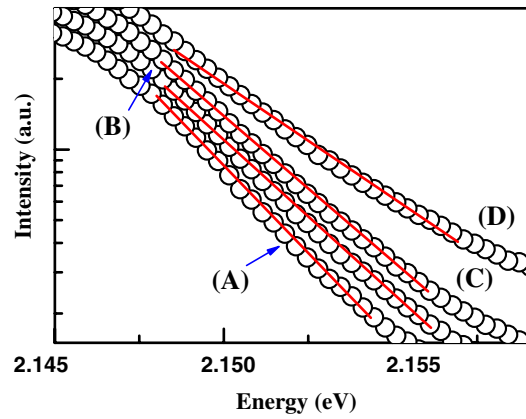


Fig. 3 Measured (open squares) and fitted (solid line) of the high-energy tail of the PL for different excitation power: (a) 353 W/cm², (b) 530 W/cm², (c) 707 W/cm², (d) 1414 W/cm²

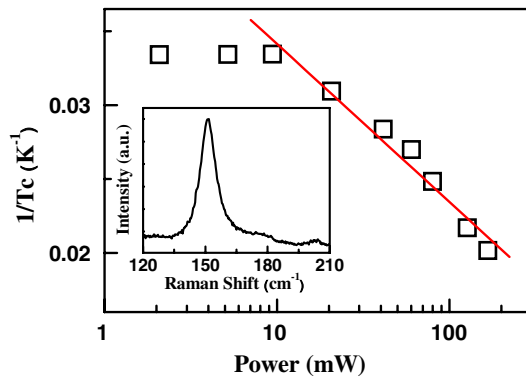


Fig. 4 The temperature dependence of PL spectra in the γ -In₂Se₃ nanorods. The inset shows the temperature dependence of peak position in PL. The solid line in the inset shows the fit according to Eq. 2

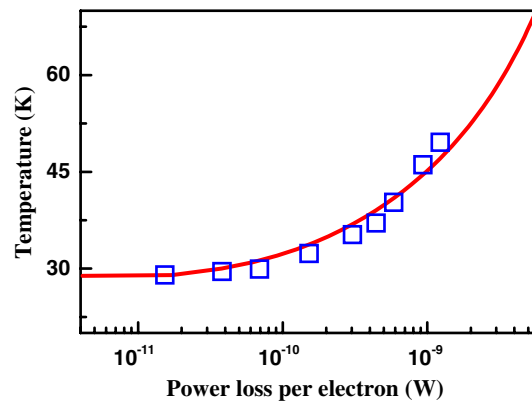


Fig. 5 The temperature dependence of PL intensity in γ -In₂Se₃ nanorods. The theoretical fit according to Eq. 3 is displayed as the dashed line

$$P(T_e) = \left(\frac{E_{LO}}{\tau_{ph}} \right) \left(\frac{e^{x_0 - x_e} - 1}{e^{x_0} - 1} \right) \left[\frac{e^{x_e/2} K_0(x_e/2)}{\sqrt{\pi/x_e}} \right], \tag{3}$$

where τ_{ph} is the effective phonon lifetime, E_{LO} is the LO-phonon energy, $x_0 = \frac{E_{\text{LO}}}{k_{\text{B}}T_i}$, $x_e = \frac{E_{\text{LO}}}{k_{\text{B}}T_e}$, and K_0 is the modified Bessel function of the order of zero. In the steady state, the power input per electron P_e is equal to the power loss to the lattice through phonon scattering. Taking values of 19 meV, $1.12 \times 10^{16} \text{ cm}^{-3}$, 2.12, 2.41 eV, $4.8 \times 10^{-6} \text{ cm}$ for E_{LO} , n , W , $h\nu_0$, d , respectively, the solid line in Fig. 4 displays the fitted T_e with the power loss per electron. Good agreement between experiments and calculations indicates that the model based on the carrier scattering by LO-phonon is able to explain the measured T_e variation with excitation power. It demonstrates again that the LO-phonon emission is the dominant energy loss mechanism in the energy relaxation processes of hot electrons in γ -In₂Se₃ nanorods.

Summary

In summary, the γ -In₂Se₃ nanorods were successfully grown on Si (111) substrates by using MOCVD. A clear room-temperature PL with the peak position of 1.95 eV was observed, corresponding to the near band edge emission. The high-energy tail of PL can be characterized by an effective T_e which increases with increasing excitation intensity. The relationship between the T_e and the electron energy loss rate can be explained by a model based on the carrier scattering by the LO-phonons.

Acknowledgments This project was supported by the National Science Council under the Grant numbers NSC 93-2112-M-033-010 and 93-2120-M-033-001, and the Center-of-Excellence Program on Membrane Technology, the Ministry of Education, Taiwan.

References

1. J. Ye, T. Yoshida, Y. Nakamura, O. Nittono, Appl. Phys. Lett. **67**, 3066 (1995). doi:[10.1063/1.114866](https://doi.org/10.1063/1.114866)
2. A. Zubiaga, J.A. Garcia, F. Plazaola, V. Munoz-Sanjose, C. Martinez-Tomas, Phys. Rev. B **68**, 245202 (2003). doi:[10.1103/PhysRevB.68.245202](https://doi.org/10.1103/PhysRevB.68.245202)
3. A.A. Homs, B. Mari, J. Appl. Phys. **88**, 4654 (2000). doi:[10.1063/1.1308066](https://doi.org/10.1063/1.1308066)
4. B. Gurbulak, Phys. Scr. **70**, 197 (2004). doi:[10.1088/0031-8949/70/2-3/020](https://doi.org/10.1088/0031-8949/70/2-3/020)
5. B. Gurbulak, M. Kundakci, A. Ates, M. Yildirim, Phys. Scr. **75**, 424 (2007). doi:[10.1088/0031-8949/75/4/008](https://doi.org/10.1088/0031-8949/75/4/008)
6. T. Stoica, R.J. Meijers, R. Calarco, T. Richter, E. Sutter, H. Luth, Nano Lett. **6**, 1541 (2006). doi:[10.1021/nl060547x](https://doi.org/10.1021/nl060547x)
7. M. Law, J. Goldberger, P. Yang, Annu. Rev. Mater. Res. **34**, 83 (2004). doi:[10.1146/annurev.matsci.34.040203.112300](https://doi.org/10.1146/annurev.matsci.34.040203.112300)
8. I.H. Choi, P.Y. Yu, J. Appl. Phys. **93**, 4673 (2003)
9. J. Shah, R.C.C. Leite, Phys. Rev. Lett. **22**, 1304 (1969). doi:[10.1103/PhysRevLett.22.1304](https://doi.org/10.1103/PhysRevLett.22.1304)
10. A. Chaiken, K. Nauka, G.A. Gibson, H. Lee, C.C. Yang, J. Wu et al., J. Appl. Phys. **94**, 2390 (2003). doi:[10.1063/1.1592631](https://doi.org/10.1063/1.1592631)
11. K.J. Chang, S.M. Lahn, J.Y. Chang, Appl. Phys. Lett. **89**, 182118 (2006). doi:[10.1063/1.2382742](https://doi.org/10.1063/1.2382742)
12. J. Shah, Solid-State Electron. **21**, 43 (1978). doi:[10.1016/0038-1101\(78\)90113-2](https://doi.org/10.1016/0038-1101(78)90113-2)
13. K. Wang, J. Simon, N. Goel, D. Jena, Appl. Phys. Lett. **88**, 022103 (2006). doi:[10.1063/1.2163709](https://doi.org/10.1063/1.2163709)